RESEARCH ARTICLE

Experimental investigation on the influence of boundary layer thickness on the base pressure and near-wake flow features of an axisymmetric blunt-based body

Alessandro Mariotti · Guido Buresti

Abstract The influence of the thickness of the boundary layer developing over the surface of an axisymmetric bluff body upon its base pressure and near-wake flow is analyzed experimentally. The model, whose diameter-to-length ratio is $d/l = 0.175$, has a forebody with an elliptical contour and a sharp-edged flat base; it is supported above a plate by means of a faired strut. The pressure distributions over the body lateral and base surfaces were obtained using numerous pressure taps, while the boundary layer profiles and the wake velocity field were measured through hot-wire anemometry. The tests were carried out at $Re = u_\infty l/v = 5.5 \times 10^5$, at which the boundary layer over the lateral surface of the body becomes turbulent before reaching the base contour. Strips of emery cloth were wrapped in various positions around the body circumference in order to modify the thickness and the characteristics of the boundary layer. The results show that increasing the boundary layer thickness causes a decrease in the base suctions and a corresponding increase in the length of the mean recirculation region present behind the body. In the spectra of the velocity fluctuations measured within and aside the wake, a dominating peak becomes evident in the region downstream of the final part of the recirculation region. The relevant non-dimensional frequency decreases with increasing boundary layer thickness; however, a Strouhal number based on the wake width and the velocity defect at a suitable reference cross section downstream of the recirculation region is found to remain almost constant for the different cases.

1 Introduction

Bluff bodies are characterized by a more or less premature separation of the boundary layer from their surface and by wakes having significant lateral dimensions and generally unsteady velocity fields. The portion of a bluff body surface lying within the separated wake is usually denoted as the *base* of the body and is subjected to low pressure values, which give a significant contribution to the total drag force acting on the body. In spite of its great interest from both the scientific and the practical points of view, the characterization of the relationship between the base pressure of a bluff body and the geometrical and fluid dynamical parameters defining a certain configuration is a complex and still open problem. The basic research activities in this field are aimed at achieving a deeper understanding of the link between the near-wake flow and the base pressure; as for the applications, one may mention the great importance of the development of methods for the reduction in the drag of road vehicles and thus of their fuel consumption.

The base pressure drag of bluff bodies is closely connected with the flow conditions in the near wake and in the separating boundary layers. In particular, if we consider a body moving in an otherwise still fluid, the work done on the fluid by the opposite of the drag force acting on the body corresponds to an increase in the sum of the kinetic and internal energies—i.e., of the total energy—of the fluid. This perturbation energy is mainly found in the wake of the body, and is a function of the amount and organization of the vorticity continuously generated over the

A. Mariotti (✉) · G. Buresti
Sezione Ingegneria Aerospaziale, Dipartimento di Ingegneria
Civile e Industriale, Università di Pisa, Via G. Caruso 8,
56122 Pisa, Italy
e-mail: alessandro.mariotti@for.unipi.it

G. Buresti
e-mail: g.buresti@ing.unipi.it

body surface and introduced in the wake. For instance, it is well known that the alternate shedding of vortices present in the wakes of two-dimensional bluff bodies gives a significant contribution to drag due to the large amount of perturbation energy corresponding to the appearance in the wake of widely separated vortices of opposite sign. This explains why any flow control method aimed at avoiding the shedding of concentrated vortices or reducing their strengths has a favorable effect on the drag experienced by a two-dimensional bluff body in cross-flow (see, e.g., Viswanath 1996; Choi et al. 2008).

The alternate vortex shedding behind two-dimensional bluff bodies is due to a strong global instability present in their wakes (see, e.g., Monkewitz 1988a) and causes large fluctuating velocities. When the characteristic Reynolds numbers are sufficiently high, velocity fluctuations are usually present also in the wakes of axisymmetric bluff bodies. However, these fluctuations are definitely smaller than those that characterize two-dimensional wakes and are connected with the appearance of a region of absolute instability in the near wake (see, e.g., Monkewitz 1988b; Pier 2008); in particular, the most unstable mode in the wake of disks and spheres is found to be an azimuthal $m = 1$ helical mode. A characteristic feature of the resulting unsteady field is the shedding of hairpin-shaped vortices, each composed of two streamwise legs and one final cross-flow portion. These vortical structures originate from the shear layers bounding the recirculation region present immediately downstream of the body and produce an instantaneously non-axisymmetric wake configuration having a symmetry plane; however, in most cases, this plane rotates randomly, thus producing an average axisymmetric wake (see, e.g., Sakamoto and Haniu 1990; Kiya et al. 2001). Nonetheless, one particular plane may be fixed by proper perturbations introduced in the wake (Grandemange et al. 2012; Vilaplana et al. 2013).

Even when regular alternate vortex shedding takes place—such as happens behind a two-dimensional bluff body—it is useful to analyze the mean recirculation region, which is found to be definitely shorter than the one present when no vortex shedding occurs and the near wake is steady. A measure of the length of this recirculation region is given by the *vortex formation length*, defined by Bearman (1965) as the distance downstream of the body base, along the wake centerline, where the rms value of the velocity fluctuations reaches a maximum. The close connection between the vortex formation distance and the end of the mean recirculation region, already pointed out by Williamson (1996), is clearly demonstrated by the results described by Balachandar et al. (1997). Furthermore, considering the data for two-dimensional blunt-based bodies in which the regular vortex shedding was modified or inhibited using either splitter plates with different

lengths or various levels of base bleed, Bearman (1967a) showed that the base pressure of a two-dimensional body decreases linearly with the increase in the inverse of the vortex formation distance. More specifically, he pointed out that "base pressure is dependent on the vortex formation distance but apparently independent of the method adopted to interfere with vortex formation." This result is consistent with the findings of Thiria et al. (2009) and Parezanovic and Cadot (2012), who showed that the drag reduction provided by a small circular cylinder placed in the near wake of a two-dimensional blunt body was connected with an increase in the length of the recirculation region, caused by a downstream movement of the maximum global instability region. Analogous results for axisymmetric wakes are less numerous, but also for this type of flow high fluctuations are normally encountered immediately downstream of the stagnation point present at the end of a mean recirculation region (see, e.g., Ilday et al. 1992). Furthermore, a decrease in drag when the recirculation region of a blunt body was lengthened by perturbing the wake through cylinders and rings was reported by Grandemange et al. (2012), who also highlighted the importance of delaying the separated shear layer instability.

The natural implication of the above results is that the base drag may be decreased if methods are devised to increase the length of the mean recirculation region. It is then important to investigate on the factors that may influence the near wake of bluff bodies. The global stability analyses of Giannetti and Luchini (2007) for cylinders and of Meliga et al. (2009) for disks and spheres provided the important result that the region where the global instability modes in the wake are more receptive to perturbations is located near the initial boundary of the recirculation region, i.e., in the vicinity of the separation point. This suggests that the conditions of the boundary layer immediately before separation may have an influence on the initial development of the separated shear layer and possibly affect the subsequent instability and the recirculation length. Indeed, some evidence exists in the literature indicating that the state and the characteristic parameters of the boundary layer developing over the lateral surface of a bluff body before its separation (i.e., over the surface of the so-called *forebody*) may influence the base pressure, particularly for bodies whose base is a sharp-edged flat surface perpendicular to the free stream. The first indication of this connection was given by Hoerner (1965), who proposed a relationship implying that increasing the forebody friction drag leads to a corresponding increase in the base pressure, and thus to a reduction in the base drag. The same idea is at the basis of the tests of Whitmore and Naughton (2002), who found a significant increase in the base pressure with increasing surface roughness of a two-dimensional flat-

sided model with a rounded leading edge. However, considering the effect of surface roughness, the base pressure variations might have been directly connected with the increasing thicknesses of the separating boundary layers rather than with the forebody drag. This was indeed explicitly done by Rowe et al. (2001), who showed that the base pressure of a thick flat plate with an elliptic leading edge increased when the thickness of the separating boundary layer was increased. The influence of the separating boundary layer over two-dimensional configurations with sharp-edged flat base was also discussed by Petrusma and Gai (1994), who found that the base pressure decreases with decreasing ratio between the separating boundary layer momentum thickness θ and the base height, with different trends according to the boundary layer being laminar or turbulent; they also suggested that an important role is played by the variations of the mean recirculation region.

As for the information relevant to axisymmetric bodies, a first indication of the possible influence of the boundary layer thickness derives from the experiments of Mair (1965), who found that the base pressure coefficient of an elongated axisymmetric body with rounded nose and sharp-edged flat base increased from -0.15 to -0.14 when the length of the body was increased in order to change the length-to-diameter ratio from $\simeq 6.0$ to $\simeq 10.0$. Indeed, it is reasonable to infer that this decrease in base suction might have been caused by the increased boundary layer thickness at separation of the longer body. A general increase in the base pressure of a flat-based cylindrical body aligned with the flow with increasing boundary layer thickness was also reported by Koh (1971), who found this dependence to be stronger for small values of the boundary layer thickness. A detailed investigation involving the variation of the boundary layer thickness was carried out by Porteiro et al. (1983) using blowing and suction through the lateral surface of a streamwise sting with circular cross section and blunt base inserted concentrically inside a nozzle of larger diameter. Again, a significant increase in the base pressure was found with increasing value of the momentum thickness of the boundary layer approaching separation. Another interesting result was obtained by Krishnan et al. (1997), who studied the effect of longitudinally oriented riblets on the base pressure of an axisymmetric body with turbulent boundary layer. They found that, contrary to their positive effect on friction drag, riblets decreased the base pressure of the body, thus increasing its base drag. In agreement with the previously described results, this finding may be explained by the decrease in the momentum thickness that is known to be produced by the addition of riblets over a surface (see, e.g., Walsh 1990).

As regards the frequency content of the wake fluctuating velocity field, Petrusma and Gai (1996) found an increase

in the Strouhal number with Reynolds number for the two-dimensional case of a plate with rounded nose and blunt trailing edge, and this finding may be associated with the corresponding decrease in the thickness of the separating boundary layer. A similar dependence on Reynolds number (and thus on the reduction in the boundary layer thickness) of the dominating frequency in the wake of axisymmetric bodies with rounded nose was described by Sevilla and Martinez-Bazan (2004) and Weickgenannt and Monkewitz (2000). More specifically, an inverse relationship between Strouhal number and boundary layer momentum thickness for an axisymmetric blunt-based cylinder was reported by Porteiro (1986), who also showed that more negative base pressures—and thus higher base drags—were associated with an increasing Strouhal number.

From the above-described limited experimental evidence, it is apparent that more research is necessary to fully understand which parameters and flow features are responsible for the ascertained connection between boundary layer characteristics, base pressure, and near-wake flow field. In the present work, the results are described of an experimental investigation carried out to analyze this connection for an axisymmetric flat-based body. This type of body was chosen because the derived information could be considered as a first step toward the possible development of methods to reduce the drag of road vehicles. The tests are restricted to the case of turbulent separating boundary layers, and their main goal is giving a contribution to understanding the physical origin of the observed influence of the boundary layer thickness.

2 Experimental setup

The tests were carried out in the closed-return, subsonic wind tunnel of the Department of Civil and Industrial Engineering of the University of Pisa, which is characterized by a circular open test section 1.1 m in diameter and 1.42 m in length, and by a free-stream turbulence level of 0.9 %. The aluminum–alloy model comprises a forebody with a 3:1 elliptical contour and a cylindrical main body with a sharp-edged base perpendicular to the axis. The model is supported above a flat plate by means of a faired strut (Fig. 1a), and its diameter and overall length are, respectively, $d = 70$ mm and $l = 400$ mm. Wind tunnel tests with axisymmetric models always pose the problem of the choice of the type of support, and none is free from drawbacks. As will be shown and discussed in next section, the chosen support implies that the flow is not symmetrical in the vertical plane, while it remains symmetrical in the horizontal plane. However, it was preferred to a rear sting support, which directly interferes with the near-wake flow development and effectively changes the free body base to

Fig. 1 Sketch of the
experimental setup. **a** Geometry
and main parameters, **b** pressure
taps and reference system
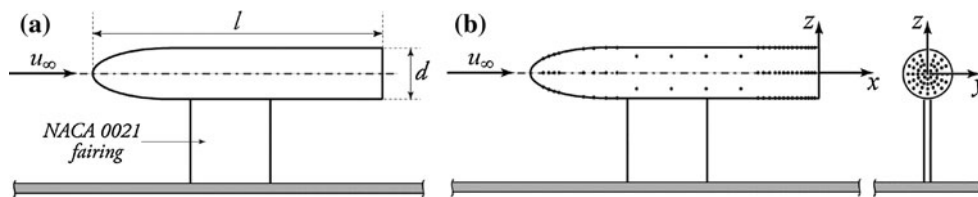
an axisymmetric backward-facing step. Furthermore, the present test conditions permit to ascertain whether, compared to what derives from the available information, the absence of axisymmetry changes—qualitatively or quantitatively—the influence of the separating boundary layer on the base pressure distribution. Finally, exact axisymmetry is not common in applications, and thus the obtained data may have a more general practical interest.

The pressures acting over the lateral and base surfaces of the body were obtained through a total of 121 pressure taps distributed over the surface of the model, 65 of which were positioned over the base (see Fig. 1b, where the adopted reference system is also shown). The taps were connected to two Pressure Systems ESP-16HD miniature electronic pressure scanners, directly positioned inside the model with the relevant output cables passing through the support fairing. The tubes connecting the taps to the pressure scanners were shorter than 100 mm, thus assuring a high frequency response (up to more than one decade higher than the maximum observed frequencies of the wake velocity fluctuations). Symmetrical pressure taps, lying on two perpendicular planes, were also present over the forebody surface and were used to accurately align the model with the free stream.

As for the velocity measurements, the boundary layer profiles and the wake velocity field were characterized using an IFA AN 1003 A.A. Lab System hot-wire anemometry module and single-wire Dantec 55P11 probes. The probes were fixed to a rear support aligned with the flow, with an approximate length of $2.5d$, which, in turn, was attached to a vertical tube connected to a computer-controlled traversing system; the probes could then be moved in the x, y, and z directions with an accuracy of 0.1 mm. After extensive preliminary tests, a sampling frequency of 2 kHz and a time length of approximately 65 s were chosen for the pressure and hot-wire signal acquisitions.

Most tests were carried out at a Reynolds number $Re = u_\infty l/\nu = 5.5 \times 10^5$, where u_∞ is the free-stream velocity.
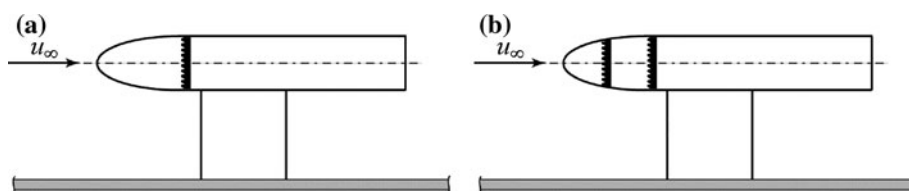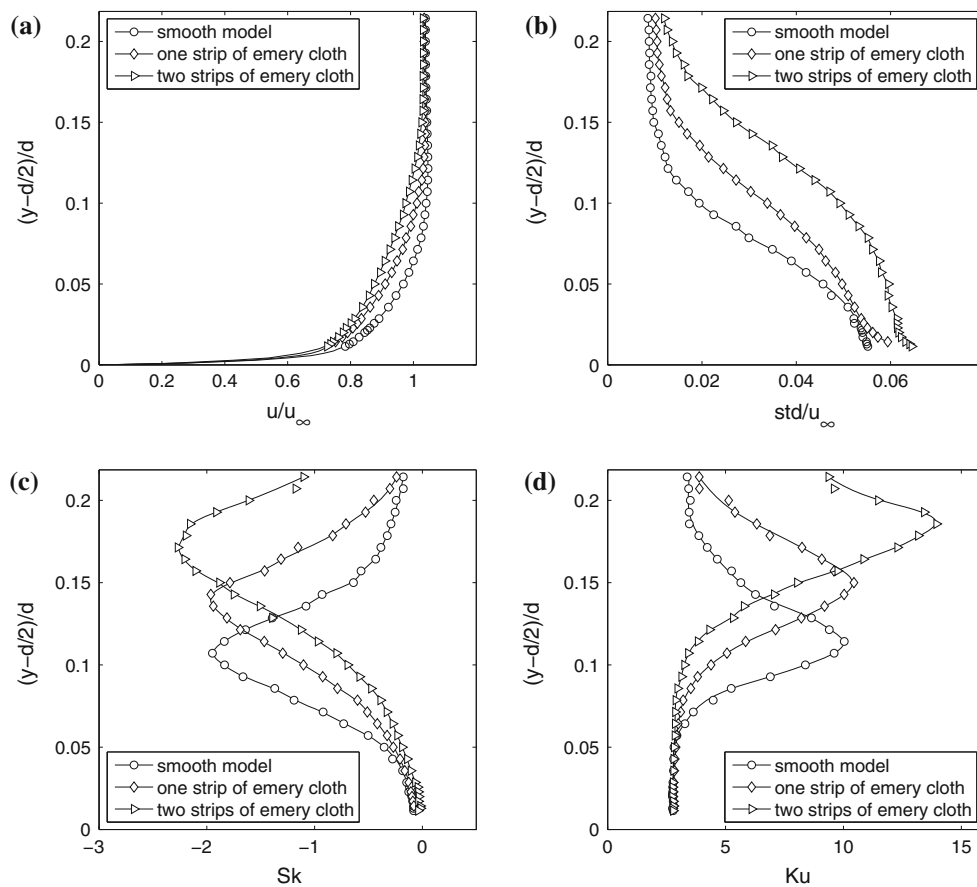
Due to the wind tunnel turbulence level, in these operating conditions the boundary layer, which remains completely attached over the lateral surface of the model, becomes turbulent before separating at the sharp-edged base contour. In order to modify the thickness and the characteristics of the boundary layer and to evaluate how they affect the base pressures, different strips of emery cloth, approximately 20 mm wide, were wrapped in various positions around the body circumference in order to move transition upstream. In particular, one strip was placed in the initial region of the constant-section main body (Fig. 2a) and another one was subsequently added over the elliptical forebody (Fig. 2b).

3 Results

3.1 Velocity measurements

The characteristics of the boundary layers over the lateral surface of the three model configurations, measured in the horizontal plane in a position $0.1d$ upstream of the base, may be deduced from Fig. 3, where the profiles of the non-dimensional mean value and of the non-dimensional higher-order central moments of the hot-wire velocity signals are reported. In all cases, both the skewness and the kurtosis—respectively, defined here as the third-order and fourth-order central moments non-dimensionalized by the third and fourth powers of the standard deviation—show a peak in the outer zone; this could be expected because the presence of such peaks at the boundary of turbulent regions with high mean shear is well documented in the literature (see, for instance, Wygnanski and Fiedler 1970 for a general two-dimensional mixing region, Fabris 1983 for wakes, Antonia and Krogstad 2001 for boundary layers, and Buresti et al. 1998 for jets). It should now be pointed out that the definition of the thickness of a boundary layer or of the edge of a wake or jet is always a conventional one,

Fig. 2 Position of the strips of
emery cloth. **a** One strip of
emery cloth, **b** two strips of
emery cloth

Fig. 3 Boundary layer velocity characteristics at $x/d = -0.1$ in the horizontal plane for the three model configurations. **a** Velocity mean value, **b** standard deviation, **c** skewness, **d** kurtosis

and is normally based on the identification of the point in space where the velocity reaches a certain percentage (99 or 95 %) of the "outer velocity." This causes non-negligible uncertainties in experimental measurements because the outer velocity—which is different from the asymptotic velocity when streamwise pressure gradients are present—is not known in advance; moreover, the edge of a shear layer belongs to a region where the velocity normal derivative is close to zero. Therefore, the negative peak of the skewness is used in this paper as a proper reference position for the edge of both the boundary layers and the wakes. This procedure provides clear and reproducible values for the thicknesses of the boundary layers and the widths of the wakes, which are closely connected with those deriving from the usual definition in terms of percentage of the outer velocity (see, e.g., Fig. 3) but are less subject to measurement uncertainty. Furthermore, using the peak of the skewness, rather than the one of the kurtosis, is preferable because shorter signals are necessary to obtain a statistically stationary value. The derived boundary layer thicknesses, δ/d, for the various configurations are summarized in Table 1, where the boundary layer displacement

Table 1 Comparison between the boundary layer characteristic thicknesses

	δ/d	δ^*/d	θ/d	H
Smooth model	0.107	0.0121	0.0086	1.41
One strip of emery cloth	0.143	0.0171	0.0121	1.41
Two strips of emery cloth	0.171	0.0194	0.0144	1.35

δ, δ^* and θ are, respectively, the thickness, the displacement thickness, and the momentum thickness of the boundary layers at $x/d = -0.1$ in the horizontal plane, $H = \delta^*/\theta$ is the shape factor

and momentum thicknesses, δ^*/d and θ/d, are also reported. The latter were obtained from the measured values, extrapolated to the wall using the viscous sub-layer law. In all conditions, the boundary layers at the end of the model lateral surface are turbulent, as can be deduced from the shape factor $H = \delta^*/\theta$, which is approximately constant around the value 1.4. On the other hand, it can clearly be seen that all the boundary layer thicknesses significantly increase with increasing surface roughness.

To characterize the near-wake flow features, hot-wire measurements along cross-flow traverses were taken at
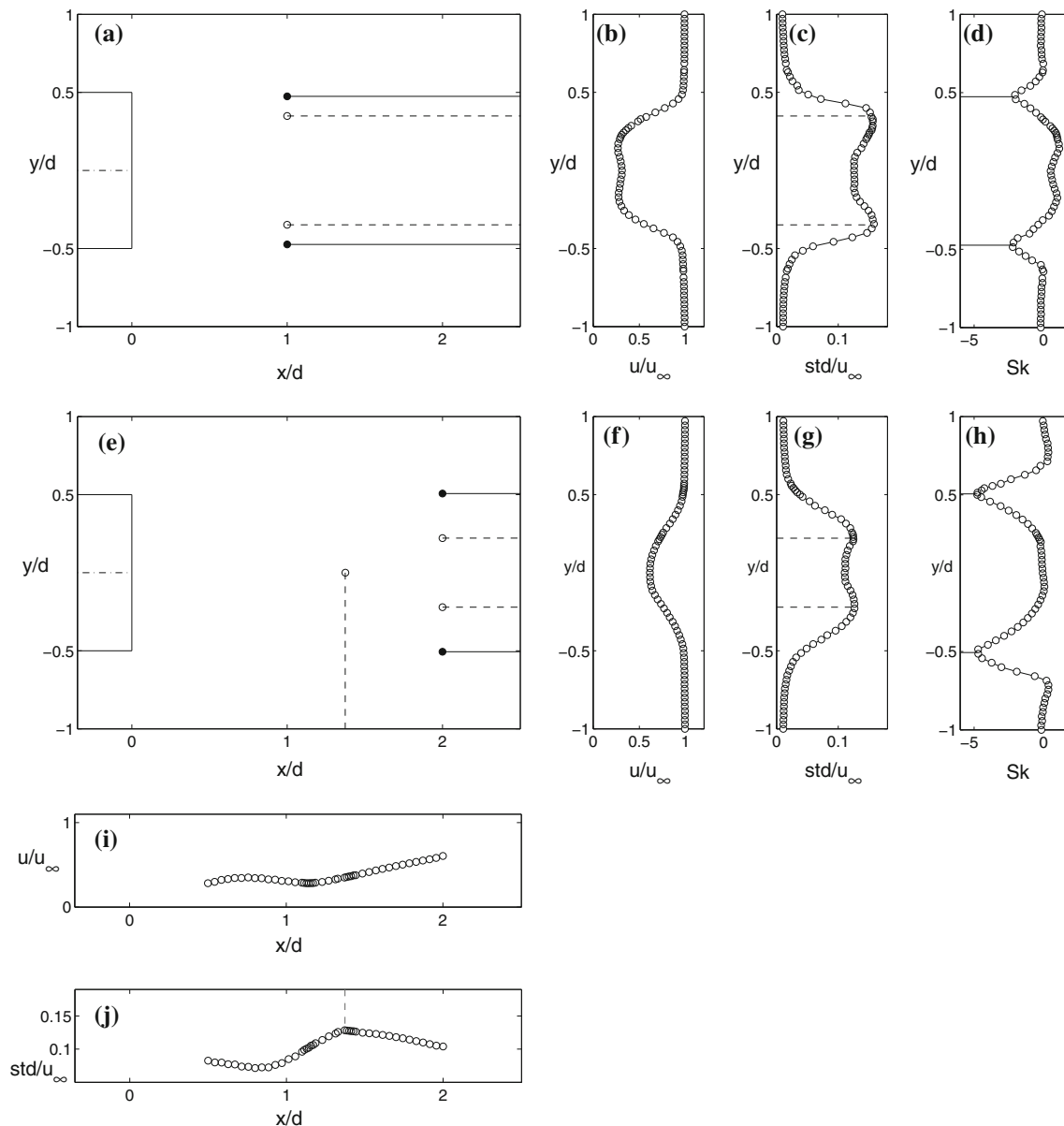
Fig. 4 a Results of hot-wire traverse at $x/d = 1$: the *black and white symbols* correspond to the peaks of the skewness and of the standard deviation, respectively; **b** non-dimensional mean velocity at $x/d = 1$; **c** non-dimensional standard deviation at $x/d = 1$; **d** skewness at $x/d = 1$; **e** results of hot-wire traverse at $x/d = 2$ and along the centerline: the *black and white symbols* correspond to peaks of the skewness and of the standard deviation, respectively; **f** non-dimensional mean velocity at $x/d = 2$; **g** non-dimensional standard deviation at $x/d = 2$; **h** skewness at $x/d = 2$; **i** non-dimensional mean velocity along the *centerline*; **j** non-dimensional standard deviation along the *centerline*

different positions downstream of the base. As an example, Fig. 4a–h shows the results along the traverses in the horizontal plane at one and two diameters downstream of the base of the smooth model. The mean velocity, the standard deviation, and the skewness profiles are shown, respectively, in Fig. 4b, c, d for the traverse at $x/d = 1$ and in Fig. 4f, g, h for the traverse at $x/d = 2$. The peaks of the standard deviation profile represent the positions of the maximum fluctuations in the wake, while the negative peaks of the skewness are representative of the wake edges;

the relevant positions are reported in Fig. 4a, e, respectively, for the planes at $x/d = 1$ and $x/d = 2$.

Hot-wire measurements were also taken along the wake centerline (Fig. 4i–j), and, as already discussed in the introduction, the peak of the standard deviation along that line was assumed to be closely related to the length of the mean recirculation region. Note that in these two figures, the obtained values are reported also for the region with $x/d < 1$, where rectification of the hot-wire signals is probably present.
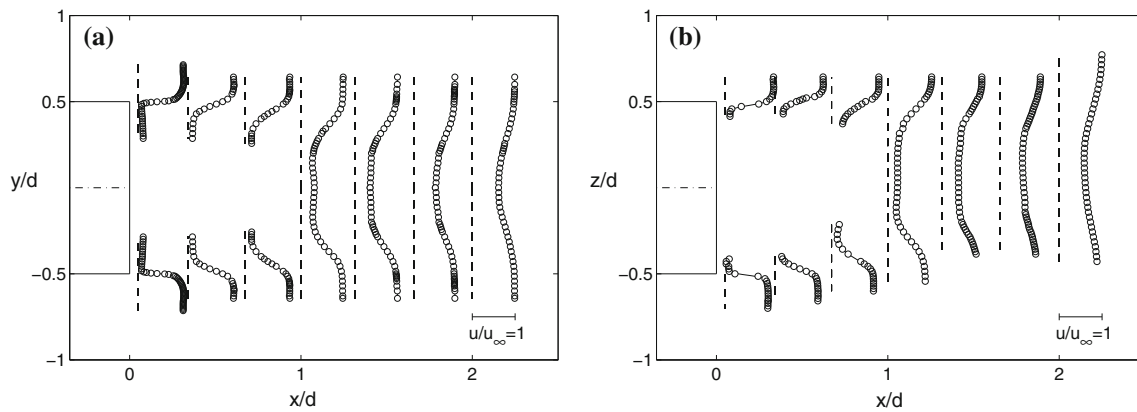
Fig. 5 Mean velocity along cross-flow traverses in the near wake. **a** Horizontal plane, **b** vertical plane
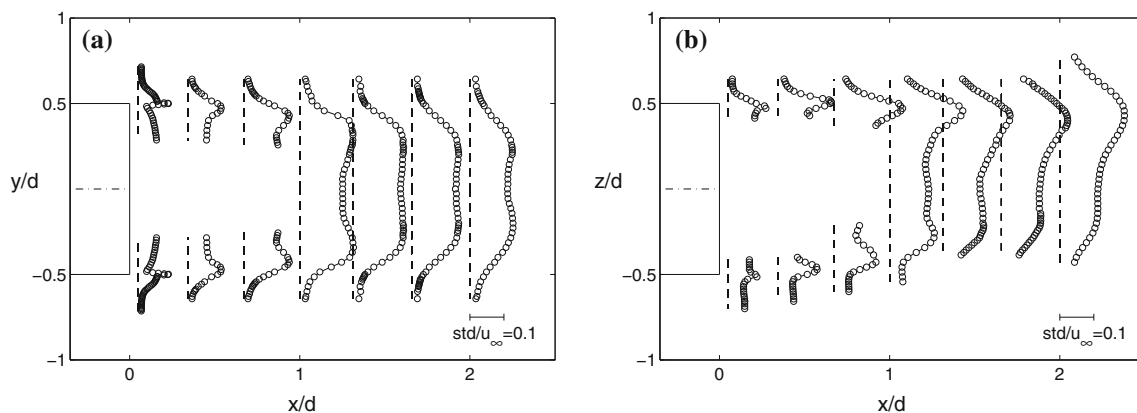

Fig. 6 Velocity standard deviation along cross-flow traverses in the near wake. **a** Horizontal plane, **b** vertical plane

Numerous measurements were taken for different cross-flow traverses in the near wake; Figs. 5 and 6 show, respectively, some of the profiles of the velocity mean value and standard deviation obtained in the horizontal and vertical planes of the smooth model. Analogous profiles are obtained for the other two cases with different surface roughness. The measured values are not shown for the positions where the hot-wire signals were presumably affected by rectification.

As can be seen in these figures and in the following Figs. 7a and 8a , the wake is symmetrical in the horizontal plane but highly non-symmetrical in the vertical plane, where, in particular, higher fluctuations are present in the upper part of the wake. It is reasonable to suppose that this flow asymmetry is most probably caused by the interference of the faired support placed below the model. Indeed, as documented by Grandemange et al. (2012), the flow past an axisymmetric elongated body with rounded nose is very sensitive to even small disturbances, which may cause the wake to become asymmetric. More specifically, Vilaplana et al. (2013) found that an asymmetric flow configuration was produced when a small vertical rod was introduced on one side of a sphere, with higher wake fluctuations in the

region opposite to the rod. This was interpreted as an indication that a preferential plane of the wake vortex shedding was stabilized by the rod, thus causing the cross-flow end portions of the vortex loops to always pass in the same region. Moreover, during the present wind tunnel tests, flow visualizations with tufts showed that a small horseshoe vortex was present around the junction between body and support; the two resulting counter-rotating vortices trailing downstream may thus be a further source of upwash velocity contributing to the upward inclination of the near wake in the vertical plane. On the other hand, the possible contribution to flow asymmetry of the plane, whose distance from the body is more than $2.2d$, should plausibly be considered definitely minor compared to the effect of the support.
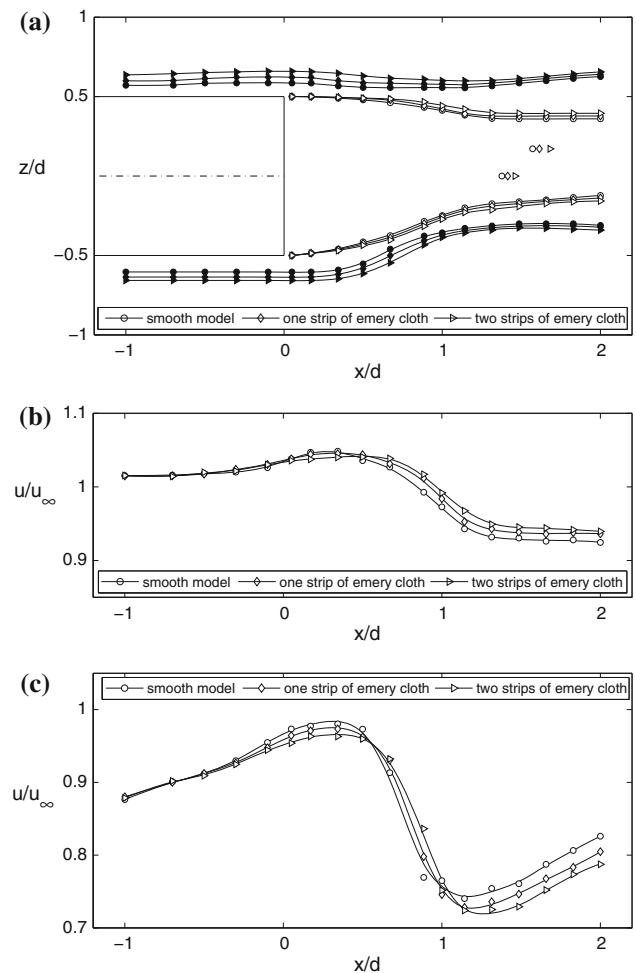
The boundary layer and wake edges (points of minimum skewness) in the horizontal plane, together with the points corresponding to the maximum fluctuations in the near wake and on the centerline, are shown for the three boundary layer configurations in Fig. 7a. As can be seen, the width of the wake initially decreases and reaches a minimum, which is probably connected with the end of the mean recirculation region. The most significant effect
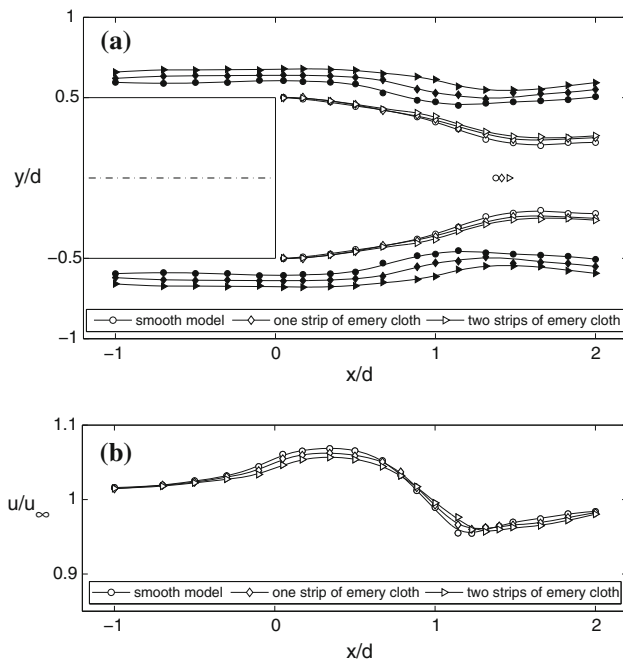
Fig. 7 Effect of the variation of the boundary layer thickness in the *horizontal plane*. **a** Boundary layer and near-wake flow features: the *black and white symbols* correspond to the peaks of the skewness and of the standard deviation, respectively, **b** Velocity distribution along the edges of the boundary layer and of the near wake

Fig. 8 Effect of the variation of the boundary layer thickness in the *vertical plane*. **a** Boundary layer and near-wake flow features: the *black and white symbols* correspond to the peaks of the skewness and of the standard deviation, respectively, **b** velocity distribution along the edges of the boundary layer and of the near wake on the *upper side*, **c** velocity distribution along the edges of the boundary layer and of the near wake on the *lower side*

caused by the increase in the boundary layer thickness, besides the predictable widening of the wake, is seen to be an increase in the length of the recirculation region. This produces a slight reduction in the curvature of the first part of the near-wake boundary, which is at first convex and then concave.

A significant effect is also found on the near-wake velocity, as can be appreciated from Fig. 7b, where the results of the longitudinal velocity measurements taken in the horizontal plane along the edges of the boundary layer and of the wake are shown. In all cases, the velocity increases in the last part of the lateral surface and along the initial boundary of the near wake, reaching a maximum approximately at $x/d = 0.3$. Subsequently, the velocity decreases and becomes lower than the free-stream velocity near the end of the recirculation region. The comparison between the various levels of surface roughness shows that the velocities are practically equal up to $x/d = -0.3$, i.e., up to slightly upstream of the base. Conversely, a lower acceleration of the flow is found downstream of this coordinate for the thicker boundary layers produced by adding the emery cloths. The reduction in the velocity is further amplified along the initial wake boundary and, consistently with the increase in the length of the recirculation region, also the subsequent deceleration is slightly delayed when the boundary layer thickness increases.

The edges of the boundary layers and wakes in the vertical plane are shown in Fig. 8a. The already mentioned asymmetry of the flow is evident in this figure: the near wake is seen to bend upwards, causing higher and lower curvatures of the lower and upper boundaries of the recirculation region, respectively. The consequence is a significant difference between the velocity variations along the upper and lower edges of the separating boundary layers and of the near wake, as can be seen from Fig. 8b, c. Note that lower starting velocities are present on the lower side due to the effect of the wake of the support. In any case, the effect of increasing the boundary layer thickness is again seen to be a lengthening of the recirculation region and a decrease in the velocity variations along its boundaries. This can be seen by the different points with maximum fluctuations obtained along the axis for the various
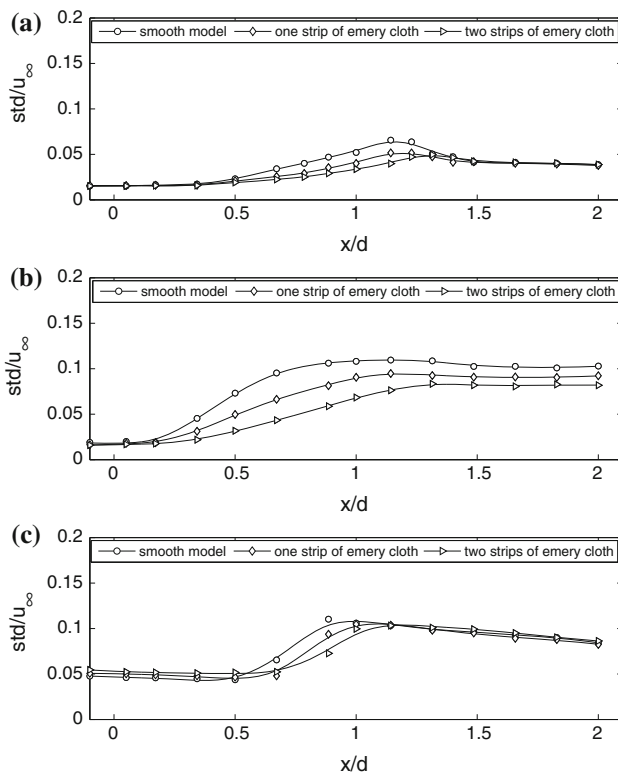
Fig. 9 Variation of the velocity standard deviation along the near-wake edges. **a** Horizontal plane, **b** vertical plane: *upper side*, **c** vertical plane: *lower side*

levels of boundary layer thickness; in order to highlight the asymmetry of the recirculation region in the vertical plane, in Fig. 8a these points are also shown along the vertical coordinate corresponding to the minimum velocity in the cross-flow traverse at $x/d = 2$.

Interesting information on the evolution of the velocity field may be obtained by analyzing the variation of the rms value of the velocity fluctuations along the curves corresponding to the near-wake edges. This variation is shown in Fig. 9a–c, respectively, for one of the two curves in the horizontal plane (which give almost equal results) and for the upper and lower curves in the vertical plane. The interest in observing these trends is that it is along these curves that the variation of the fluctuations connected with the shear layer instability—and thus with the dynamics of the consequent concentrations of vorticity—may best be identified. Starting the analysis from the upper wake edge in the vertical plane, for which maximum variations are found, it is seen from Fig. 9b that the fluctuations start increasing at a certain position, and this is consistent with the beginning of the instability along the boundary of the recirculation region. The effect of increasing the boundary layer thickness is then seen to be a delay of the rise in the fluctuations, and, thus, presumably, a corresponding downstream movement of the shear layer instability, in

connection with the already observed lengthening of the recirculation region. The trend along the lateral edge in the horizontal plane is similar (see Fig. 9a) but with smaller and delayed variations. As for the lower-side edge in the vertical plane, Fig. 9c shows that the variations are similar to those on the lateral plane, but are less separated. Furthermore, it is seen that the more upstream values of the fluctuations are higher along this curve, once again due to the effect of the wake of the support. These differences between the trends along the various wake edges are actually consistent with the already suggested stabilization of a preferential vertical symmetry plane for the shedding of hairpin vortices due to the interference of the support.

The above hypothesis on the downstream configuration of the wake is further substantiated by the analysis of the variation of the kurtosis of the velocity signals along the curves corresponding to the cross-sectional maxima of the fluctuations, which are shown in Fig. 10a–c. Indeed, when high levels of fluctuations are present, the value of the kurtosis may give clues on the origin of those fluctuations. We have already seen that high values of the kurtosis indicate the occurrence of sporadic velocity values distant from the mean. Conversely, when the kurtosis is significantly lower than the Gaussian value of 3, the fluctuations have fewer extreme values and are nearer to a sinusoid (whose kurtosis is equal to 1.5). This usually indicates that the detected large fluctuations are dominated by the velocities induced by the regular passage of concentrated vortical structures, as happens, for instance, due to the alternate vortex shedding in the wake of a two-dimensional body in cross-flow. For the present measurements, most values are only slightly lower than 3, except for those obtained along the maximum-rms curve on the upper side of the vertical plane (Fig. 10b), where the kurtosis decreases significantly—reaching a value of the order of 2—starting from a position that roughly corresponds to the increase in the fluctuations shown in Fig. 9b. A lower decrease in the kurtosis is also found along the lower-side curve in the vertical plane (Fig. 10c), whereas only very small variations are present in the horizontal plane (Fig. 10a). These results clearly suggest that the generation and passage of the cross-flow vorticity regions corresponding to the ends of the hairpin vortices occur prevalently along the upper part of the wake. Furthermore, the influence of the increase in the separating boundary layer thickness on the production process of these structures is also confirmed by the delayed variation of the kurtosis.

3.2 Pressure measurements

The variations of the pressure coefficient along the last portion of the lateral surface of the body is shown for the different analyzed configurations in Fig. 11a for the

Fig. 10 Comparison between
the values of the kurtosis along
the peaks of the velocity
standard deviation. **a** Horizontal
plane, **b** vertical plane: *upper
side*, **c** vertical plane: *lower side*
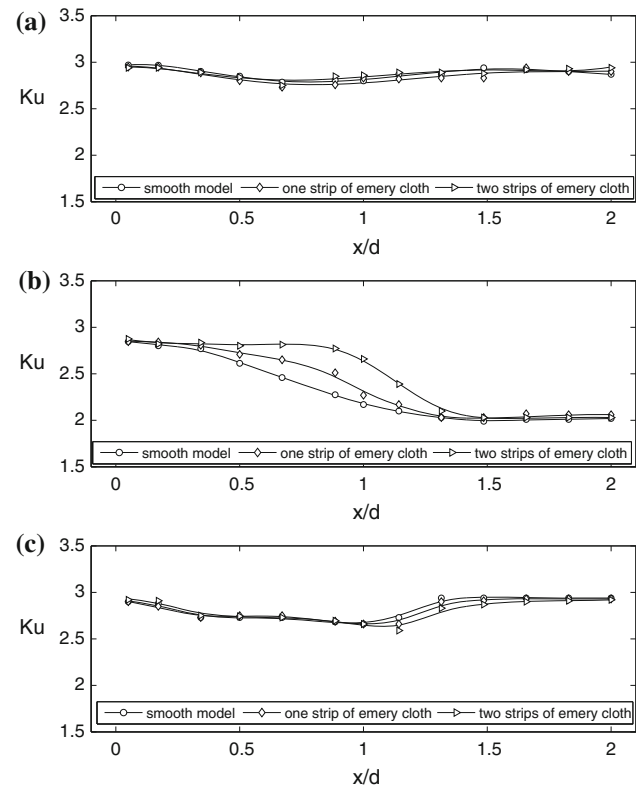
horizontal plane and in Fig. 11b for the vertical plane. As is apparent, in all cases the pressure significantly decreases by approaching the base contour, and this is consistent with the already described acceleration occurring outside the boundary layer in that region. Furthermore, in the vertical plane, a significant difference exists between the trends of the upper and lower part, again in agreement with the variations of the velocity in the near-wake boundaries: a higher increase in the suctions is indeed present on the lower side, where the curvature of the boundary of the recirculation region is higher (see Fig. 8a). As for the effect of the increase in the boundary layer thickness, it is found to be visible only in the last part of the lateral surface: the pressures are practically identical for the smooth and the two rough models upstream of the coordinate $x/d = -0.3$, whereas more downstream lower suctions are found in the configurations with thicker boundary layers. The last measurement point on the lateral surface is located at $x/d = -0.07$, and in Fig. 11 dashed lines show the extrapolations of the obtained data up to the base contour. This permits a clearer assessment of the differences between the various cases, which, however, become more significant and evident over the base, as can be appreciated from Fig. 12. In the horizontal plane (Fig. 12a), the pressure is approximately symmetrical over the base and the maximum increases in the pressure caused by the increase in the boundary layer thickness are found in the center of the base, where the largest suctions are always present. Conversely, due to the already discussed flow

asymmetry caused by the support interference, in the vertical plane (Fig. 12b) higher suctions are present on the lower part, where the greatest effects of the boundary layer thickness are also displaced.

A more immediate idea of the variations in base pressure produced by increasing the boundary layer thickness may probably be obtained from the comparison between the global distributions of the pressure over the body base found for the various cases, which are shown in Fig. 13 by using gray levels and isolines, considering the region of the base where pressure taps were present (with radial coordinate lower than $0.4d$). By associating the pressure values measured on each of the pressure taps to a surface sector, the average base pressure coefficients were then estimated for the various surface conditions. If the outer annulus where no measurements had been taken is neglected, the results of this evaluation are $C_p = -0.160$ for the lower boundary layer thickness, $C_p = -0.153$ for the intermediate boundary layer thickness, and $C_p = -0.146$ for the higher boundary layer thickness. The corresponding increases in the base-averaged pressure coefficient (and thus reductions in base drag) for the two thicker boundary layers compared to the smooth model are then 4.4 and 8.7 %, respectively. On the other hand, if the measured values are extrapolated to the base contour (as shown in Fig. 12b), the above numerical values vary only slightly, and the base pressure increases become 4.1 and 8.2 %, respectively.

Fig. 11 Comparison between the pressure distributions over the last portion of the lateral surface. In the vertical plane, the *black* and the *white symbols* correspond to the upper side and the lower side, respectively. **a** Horizontal plane, **b** vertical plane
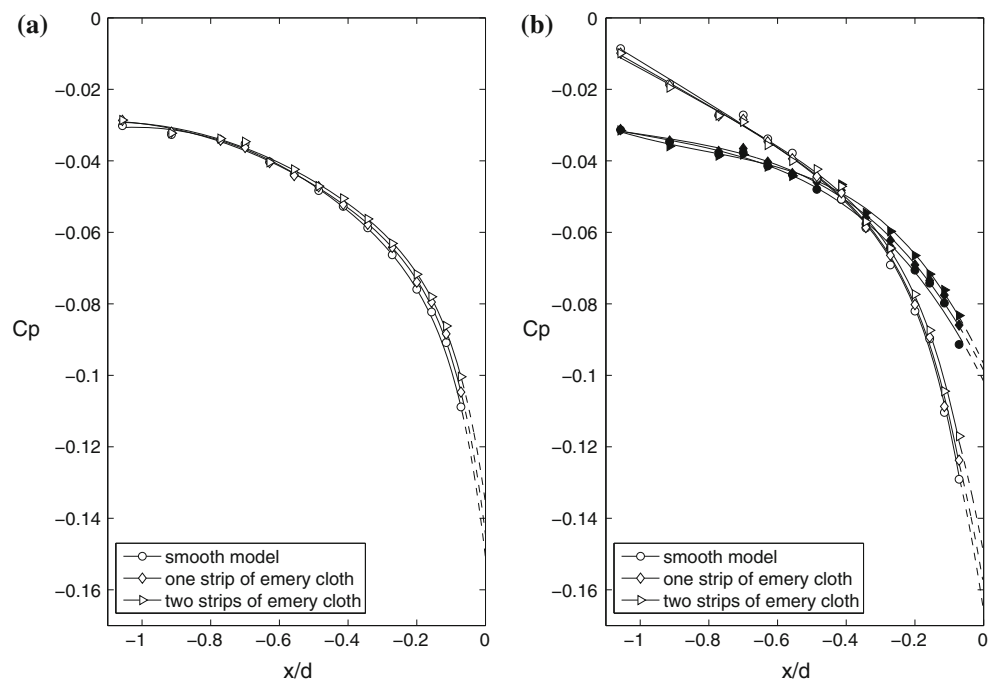
Fig. 12 Comparison between the base pressure distributions. **a** Horizontal plane, **b** vertical plane
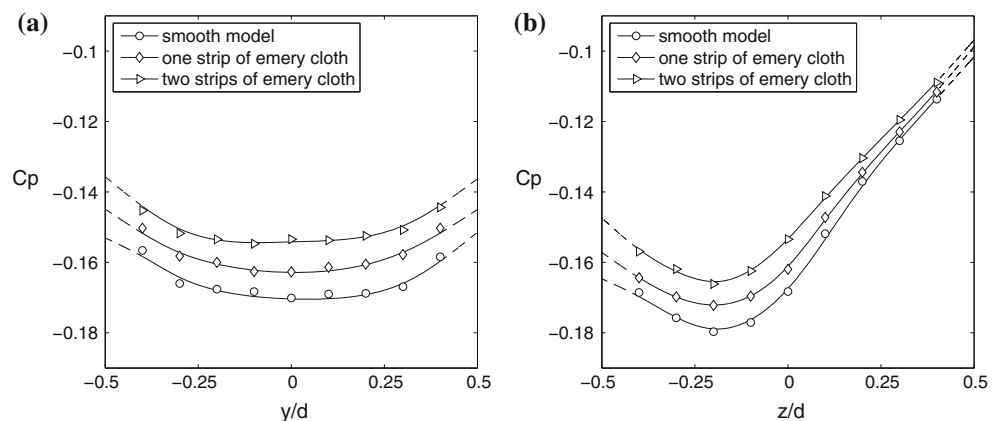
## 3.3 Frequency analysis of the wake velocity signals

The spectral content of the velocity fluctuations in the near-wake field was characterized for the different levels of boundary layers thickness. To this end, techniques based on the wavelet transform were preferred to conventional Fourier analysis. In particular, the spectra described in the following were derived by integration in time of the wavelet maps obtained by employing the complex Morlet wavelet, $\Psi(t) = e^{iw_0 t}e^{-t^2/2}$, using a central frequency $\omega_0 = 6\pi$ in order to enhance the frequency resolution. This permits to obtain spectra that are smoother than the Fourier ones and well defined from the mathematical point of view. Mean spectra were obtained by averaging the wavelet spectra of 10 different velocity signals in the same position.

The mean wavelet spectra of the velocity signals, measured for the smooth model $0.07d$ outside the wake edges

in different longitudinal positions in the interval $x/d = 0.05$–2, are presented in Fig. 14. The frequencies are expressed in non-dimensional form through a Strouhal number based on the model diameter and the free-stream velocity, $St = fd/u_\infty$. As can be observed, a clear dominating peak was found in the spectra for $x/d \geq 0.5$, with increasing intensity approaching the region just downstream of the end of the recirculation region, where a well-defined frequency peak at $St \cong 0.26$ is present. Peaks with the same dominating frequency were also found in different positions within and aside the wake. As could be ascertained by repeating the tests at different velocities, the relevant frequency is directly related to the free-stream velocity and is thus plausibly connected with the flow dynamics.

The comparison between the values of the Strouhal number corresponding to the dominating frequencies for
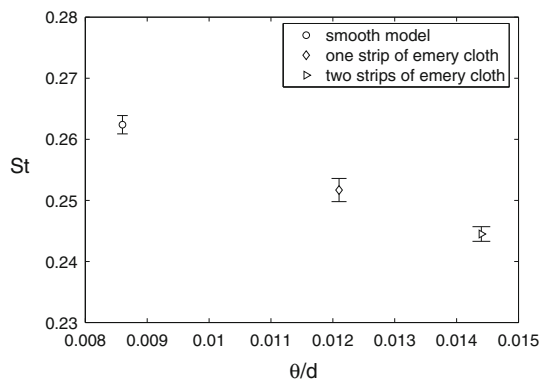
Fig. 13 Distributions of the pressure coefficient over the base. The distance between the isolines is $\Delta C_p = 0.005$. **a** Smooth model, **b** one strip of emery cloth, **c** two strips of emery cloth
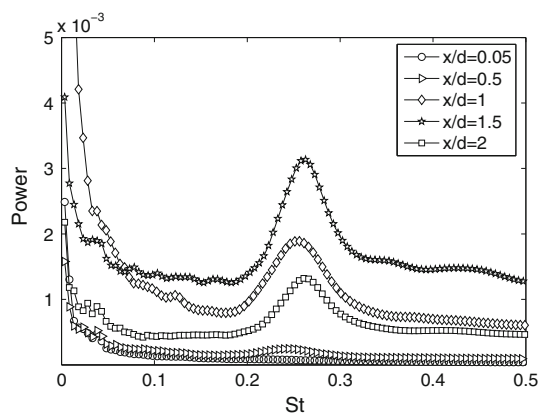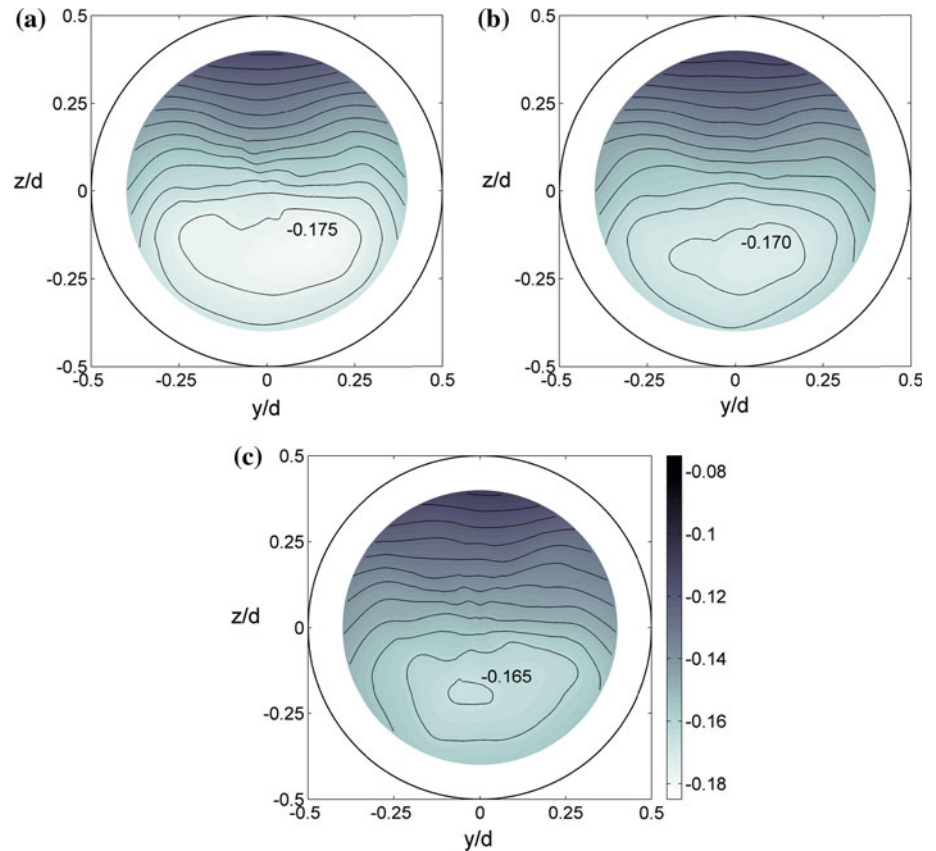

Fig. 14 Wavelet spectra of the velocity signals outside the wake edges in different longitudinal positions for the smooth model

check that this result does not change significantly if the virtual increase in the body diameter is taken into account by adding twice the displacement thickness of the separating boundary layers. As for the values of the Strouhal numbers available in the literature for similar bodies, Morel (1979) found $St \cong 0.22$ for a body shape and at Reynolds numbers comparable to those used in the present investigation. However, the momentum thickness near separation was higher ($\theta/d \cong 0.018$), probably because the model had a long front cylindrical extension with a diameter equal to approximately $d/3$. Furthermore, the free-stream turbulence level was significantly lower (less than 0.1 %). Both these instances, together with the probably higher level of asymmetry of the present configuration, might explain the different values of the Strouhal number. Lower values of the Strouhal number were also found by Porteiro (1986), but with lower Reynolds numbers and higher thicknesses of the separating boundary layer. On the other hand, the values reported by Sevilla and Martinez-Bazan (2004) vary from 0.23 to 0.26 with increasing Reynolds number, and even higher values were predicted theoretically by Weickgenannt and Monkewitz (2000). Finally, the numerical value obtained in the present investigation for the thickest boundary layer is not far from the one ($St = 0.246$) found by Calvert (1967) for a cylindrical body with an ellipsoidal nose.

the three different boundary layer thicknesses, obtained outside the wake edges at $x/d = 2$, is shown in Fig. 15. In the figure, the bars represent the 95 % confidence intervals of the Strouhal number, based on the uncertainty derived from the standard deviation of the peak frequency values obtained from the 10 spectra. From this figure, it is clear that the dominating frequency decreases with increasing momentum thickness of the separating boundary layer. A similar behavior is found also for the hot-wire velocity signals measured at $x/d = 1$ and $x/d = 1.5$. It is easy to

Fig. 15 Variation of the Strouhal number of the velocity signals with the boundary layer momentum thickness. The frequencies are measured at $x/d = 2$ and θ in the horizontal plane at $x/d = -0.1$
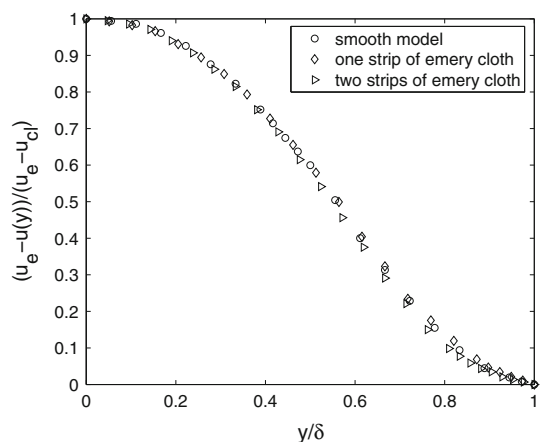

Fig. 16 Non-dimensional velocity defect at $x/d = 2$ as a function of y/δ for the different boundary layer thicknesses

A deeper scrutiny of the flow development in the near wake was then carried out in the attempt to verify whether the frequency variation could be connected with the trend of other flow quantities. An interesting finding arising from this analysis is that, downstream of the recirculation region, the velocity profiles for the different configurations become similar if they are expressed in terms of suitably chosen non-dimensional coordinates. In particular, for each cross section at a longitudinal coordinate x/d in the horizontal plane, we may define u_{cl} as the velocity at the center of the wake and u_e as the velocity at the coordinate $y = \delta$ of the lateral edge of the wake, identified through the skewness negative peaks. By using these quantities, the data for all the different degrees of surface roughness collapse to a single curve when the profile of the non-dimensional lateral velocity defect $(u_e - u(y))/(u_e - u_{cl})$ is plotted as a function of the coordinate y/δ (see Fig. 16, which corresponds to the cross section at $x/d = 2$). A remarkable similarity of the non-dimensional velocity profiles, for cross sections

starting slightly downstream of the end of the recirculation region, was also reported by Calvert (1967) for the wake of several axisymmetric models and by Porteiro and Perez-Villar (1996) for a blunt-based sting with boundary layer suction or base bleed.

An attempt was then made to study the possibility of defining a modified Strouhal number that might be constant for the different boundary layers. The idea of devising universal numbers to connect the frequency of the wake fluctuations with suitable reference velocities and lengths was first introduced by Roshko (1954) for the fluctuations caused by the alternate vortex shedding from different two-dimensional bodies. Subsequently, other parameters were proposed, with various degrees of success, by several investigators (see, e.g., Bearman 1967b; Griffin 1978; Buresti 1983), and the idea was also extended to axisymmetric bodies by Calvert (1967). Most of these numbers are, essentially, Strouhal numbers in which the reference velocity is derived from the base pressure—and is thus connected with drag—and the reference length is some measure of the "width" of the wake, often characterizing the end of the recirculation region. Considering the above-described results of the present investigation, good candidates for the reference velocity and length seemed to be the values of the wake velocity defect—which is also linked to the body drag—and of δ at a suitable reference cross section. On the basis of the previous attempts in the literature, the sensible choice for the latter seemed to be the one at the axial coordinate corresponding to the maximum of the rms fluctuations on the axis, which we have seen to be strictly connected with the length of the recirculation region. However, in that cross section some hot-wire rectification might be expected near the axis. Therefore, it was decided to use three more downstream cross sections, separated by the same distance from the positions of the maximum-rms values that are visible, for the three configurations, in Fig. 7a. The three chosen cross sections were then the ones at $x/d = 1.915$, $x/d = 1.955$, $x/d = 2$, respectively, for the three increasing boundary layer thicknesses. The values of δ and of the velocity defects at these cross sections were then used to evaluate the modified Strouhal number $St_\delta = f\delta/(u_e - u_{cl})$, and its values for the three different boundary layers are reported in Fig. 17; note that the uncertainty bars in this figure are slightly larger than those in Fig. 15 because the uncertainty in the value of δ is also taken into account. As can be seen, the variations of the modified Strouhal number are much smaller than those of St, witnessing a possible connection between the dominating frequency of the wake velocity fluctuations and the characteristic quantities of the shear layer at corresponding cross sections downstream of the recirculation region.
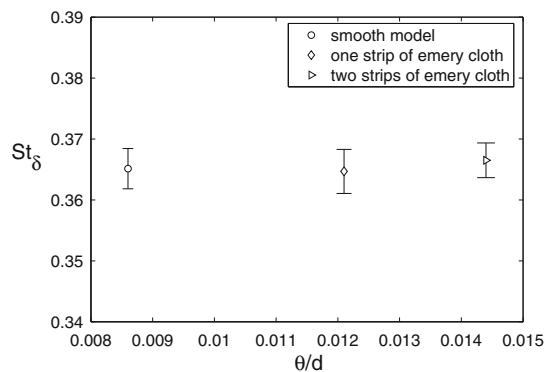
Fig. 17 Variation of the modified Strouhal number, St_δ, with the boundary layer momentum thickness. The frequencies, the velocity defects, and the wake widths are measured at $x/d = 1.915$, $x/d = 1.955$, and $x/d = 2$, respectively, for increasing θ

4 Discussion and conclusions

In this work the results have been described of a wind tunnel investigation carried out to study the influence of the characteristics of the boundary layer developing over the surface of an axisymmetric bluff body upon its base pressure and near-wake flow features. The tests were carried out at a Reynolds number for which the boundary layer over the smooth lateral surface of the body becomes turbulent before reaching the base contour. Different strips of emery cloth were wrapped in various positions around the body circumference in order to modify the thickness and the characteristics of the boundary layer. The increase in the boundary layer thickness was found to significantly reduce the base suctions and thus the pressure drag of the body. This result agrees with previous ones for two-dimensional and axisymmetric bodies, in spite of the significant flow asymmetry in the vertical plane caused by the body support. Therefore, the present data confirm that even in these conditions, which are probably nearer to the ones that may occur in practical applications, increasing the boundary layer thickness may be beneficial as regards the base drag of a bluff body.

Near-wake velocity measurements were also taken, and the obtained results suggest that the increase in base pressure with increasing boundary layer thickness is plausibly connected with an ascertained increase in the length of the mean recirculation region present behind the body. Indeed, the velocities at the edge of the separating boundary layers and of the initial part of the near-wake external boundary were also found to decrease, in agreement with the observed trends of the pressure both on the lateral surface and on the base of the body. These velocity variations may be associated with a decrease in the convex curvature of the initial boundary of the recirculation region, where the pressures may also be expected to increase with

increasing boundary layer thickness. The observed experimental data are then consistent with the reasonable supposition that the pressures acting over the body base are closely connected with the values of the velocity and pressure outside the separating boundary layer and on the first part of the contour of the recirculation region.

As regards the possible relationship between the mean flow field and the mean drag acting on the body in a situation in which the wake flow is actually unsteady, one may note that the flux of vorticity into the wake and the base pressure coefficient vary as the square of the velocity outside the separating boundary layer; consequently, both these quantities depend also on the square of the velocity fluctuations. However, if the mean square value of the fluctuations is small compared to the square of the mean value of the velocity, then the mean base pressure and vorticity flux are mainly dependent on the mean velocity field. This leads to a possible difference between two-dimensional bluff bodies, characterized by the regular shedding of strong and highly concentrated vortices in their wakes—and thus by significant velocity fluctuations—and axisymmetric bodies, for which the shed vortical structures are weaker and the consequent fluctuations are definitely smaller. Therefore, for axisymmetric bodies the shape and the dimensions of the mean recirculation region may be expected to have a higher direct relevance as regards the value of the mean drag. However, it is also true that velocity fluctuations do have an influence on the length of the recirculation region because, as pointed out in the introduction, the position of the onset of the instability in the separated shear layers controls the axial coordinate at which the end point of the recirculation occurs. The importance of the fluctuating velocity field is also demonstrated by the results of Rind and Castro (2012), who showed that increasing the free-stream turbulence level produces a reduction in the recirculation length of a circular disk and a simultaneous drag increase, and ascribed this effect to the increased entrainment caused by the increase in turbulence level. Therefore, any flow feature that may cause a delay of the instability of the shear layer bounding the recirculation region may be expected to cause an increase in its length. The present results on the trends of the velocity central moments along the near-wake boundary seem to suggest that this is indeed one of the effects of the increase in the boundary layer thickness, in agreement with the high receptivity of the shear layer instability to perturbations in the separation region. The origin of this effect may perhaps be connected with the decrease in the maximum normal gradient—and thus in the maximum vorticity value—existing within the separating boundary layer.

In spite of the above highlighted importance of the configuration of the mean recirculation region, the mean

base pressure and velocity fields are probably associated in a more complex way with the detailed characteristics of the mean and unsteady velocity and vorticity fields that are present in the more downstream region of the wake. In this respect, any physical interpretation as regards the influence of the separating boundary layer thickness must be consistent with the fundamental equations of fluid dynamics and with the derived relations. In particular, as already pointed out in the introduction, in a reference system moving with the free-stream velocity the work done on the fluid in unit time by the opposite of the drag force is directly connected with the total energy perturbation, i.e., with the time variation of the kinetic and internal energies in the flow field. Therefore, the present results indicate that lower total energy is being introduced in the wake in unit time when the boundary layer thickness is increased. It is then useful to recall that the perturbation energy is an increasing function of the amount and concentration of the vorticity continuously shed into the wake. Furthermore, the importance of the vorticity field is also highlighted by the fact that any fluid dynamic force may be expressed in terms of the time variation of the moment of vorticity (see, e.g., Wu 1981; Wu et al. 2006; Buresti 2012). Thus, the drag is linked to the time variation of the axial moment of vorticity, which, in turn, is essentially connected with the vorticity being introduced in the wake downstream of the recirculation region. When trying to synthesize the available evidence on the factors influencing drag, all these issues must then be carefully considered in order to attain a deeper comprehension of the physical mechanisms that are at the basis of the observed results.

In the present tests, the presence of the model support caused a flow asymmetry, which was shown to be probably due to the stabilization of a vortex shedding pattern having a predominantly vertical symmetry plane, with the cross-flow portions of the vortices displaced toward the wake upper part. Evidence of this stabilization derives also from the trends of the kurtosis of the velocity fluctuations along the upper-side curves corresponding to the maxima of the rms fluctuations in the vertical plane. It might then be reasonable to suppose that the present asymmetric configuration produces a wake structure with a more regular vortex shedding than would occur for a randomly varying vortex shedding orientation, and thus probably associated with higher mean perturbation energy and drag. It may also be noted that this asymmetric flow configuration produces a negative lift acting on the body, as witnessed by the pressure distribution over the final portion of the lateral surface of the body. Therefore, one might correlate part of the drag acting on the body with the value of the lift force that it experiences. However, the origin of this additional drag corresponds, in any case, to an increased perturbation energy, plausibly connected with a higher organization of

the vortical structures shed into the wake. Thus, also this part of the drag—together with the associated negative lift—may be considered to be reduced by the increase in boundary layer thickness.

A further result of the present investigation is that the variation in the thickness of the separating boundary layer may also have a significant influence on the velocity fluctuations observed downstream of the recirculation region, whose dominating frequency was found to decrease with the increase in the boundary layer thickness. However, a Strouhal number based on a characteristic measure of the wake width and on the velocity defect at a suitable reference axial coordinate, linked to the end of the recirculation region, was found to remain substantially constant for all the considered cases. This again confirms the importance of the flow field features at the end and immediately downstream of the mean recirculation region, where the shedding of hairpin vortices originates. Furthermore, the constancy of the modified Strouhal number suggests that the frequency of this shedding is proportional to the velocity gradient in the cross-flow direction at the reference cross section.

A final observation arising from the present results is that, even for bluff bodies with fixed separation points, the sensitivity to the boundary layer thickness and to the turbulence level may be a source of scatter in experimental data for drag coefficients; indeed, increasing the former increases the recirculation length while the opposite occurs for increasing turbulence. Consequently, the rate of increase in the base pressure with increasing thickness of the separating boundary layer might probably not be the same for laminar and turbulent boundary layers, as already suggested by Rowe et al. (2001); this also implies that the results of the experimental investigations may be influenced by the value of the Reynolds number based on the length of the body portion with attached boundary layer.

In any case, the full comprehension of all the physical mechanisms influencing the base drag of a bluff body is still far from being achieved, and much more research work is thus indispensable. For instance, it remains not clear whether the effect on the base pressure is connected with the variation of all the boundary layer characteristic thicknesses or only of certain ones. Indeed, considering that in the present investigation all the thicknesses varied consistently when the emery cloths were added over the surface, the only obtained output in this direction is that the shape factor should not be a controlling parameter. It would then be important to study the effect of changing only the value of single parameters, while keeping the other ones unaltered. This is certainly not simple to obtain in experiments, whereas it might be much more easily feasible through numerical simulations; on the other hand, the latter are not yet capable of accurately predicting the

wake flow field of bluff bodies for the high Reynolds numbers that are usually encountered in the applications. Therefore, a synergic use of various types of numerical simulations and of experiments might probably represent the most fruitful way of exploiting, in future investigations, the currently available research tools.

References

Antonia RA, Krogstad PÅ (2001) Turbulence structure in boundary layers over different types of surface roughness. Fluid Dyn Res 28:139–157

Balachandar S, Mittal R, Najjar FM (1997) Properties of the mean recirculation region in the wakes of two-dimensional bluff bodies. J Fluid Mech 351:167–199

Bearman PW (1965) Investigation of the flow behind a two-dimensional model with blunt trailing edge and fitted with splitter plates. J Fluid Mech 21:241–255

Bearman PW (1967a) The effect of base bleed on the flow behind a two-dimensional model with a blunt trailing edge. Aeronaut Q 18:207–224

Bearman PW (1967b) On vortex street wakes. J Fluid Mech 28:625–641

Buresti G (1983) Appraisal of universal wake numbers from data for roughened circular cylinders. J Fluids Eng 105:464–468

Buresti G (2012) Elements of fluid dynamics. Imperial College Press, London

Buresti G, Petagna P, Talamelli A (1998) Experimental investigation on the turbulent near-field of coaxial jets. Exp Therm Fluid Sci 17:18–36

Calvert JR (1967) Experiments on the low-speed flow past cones. J Fluid Mech 27:273–289

Choi H, Jeon WP, Kim J (2008) Control of flow over a bluff body. Annu Rev Fluid Mech 40:113–139

Fabris G (1983) Higher-order statistics of turbulent fluctuations in the plane wake. Phys Fluids 26:1437–1445

Giannetti F, Luchini P (2007) Structural sensitivity of the first instability of the cylinder wake. J Fluid Mech 581:167–197

Grandemange M, Gohlke M, Parezanovic V, Cadot O (2012) On experimental sensitivity analysis of the turbulent wake from an axisymmetric blunt trailing edge. Phys Fluids 24:035106

Griffin OM (1978) A universal number for the "locking-on" of vortex shedding to the vibrations of bluff cylinders. J Fluid Mech 85:591–606

Hoerner SF (1965) Fluid dynamic drag. Hoerner Fluid Dynamics, Bakersfield, USA

Ilday Ö, Acar H, Elbay MK, Atli V (1992) Wakes of three axisymmetric bodies at zero angle of attack. AIAA J 31:1152–1154

Kiya M, Ishikawa H, Sakamoto H (2001) Near-wake instabilities and vortex structures of three-dimensional bluff bodies: a review. J Wind Eng Ind Aerodyn 89:1219–1232

Koh JCY (1971) A new wind-tunnel technique for providing simulation of flight base flow. J Spacecr Rockets 8:1095–1096

Krishnan V, Viswanath PR, Rudrakumar S (1997) Effect of riblets on axisymmetric base pressure. J Spacecr Rockets 34:256–258

Mair WA (1965) The effect of a rear-mounted disc on the drag of a blunt-based body of revolution. Aeronaut Q 16:350–360

Meliga P, Chomaz JM, Sipp D (2009) Unsteadiness in the wake of disks and spheres: instability, receptivity and control using direct and adjoint global stability analyses. J Fluid Struct 25:601–616

Monkewitz PA (1988a) The absolute and convective nature of instability in two-dimensional wakes at low Reynolds numbers. Phys Fluids 31:999–1006

Monkewitz PA (1988b) A note on vortex shedding from axisymmetric bluff bodies. J Fluid Mech 192:561–575

Morel T (1979) Effect of base cavities on the aerodynamic drag of an axisymmetric cylinder. Aeronaut Q 30:400–412

Parezanovic V, Cadot O (2012) Experimental sensitivity analysis of the global properties of a two-dimensional turbulent wake. J Fluid Mech 693:115–149

Petrusma MS, Gai SL (1994) The effect of geometry on the base pressure recovery of segmented blunt trailing edges. Aeronaut J 98:267–274

Petrusma MS, Gai SL (1996) Bluff body wakes with free, fixed, and discontinuous separation at low Reynolds numbers and low aspect ratio. Exp Fluids 20:189–198

Pier B (2008) Local and global instabilities in the wake of a sphere. J Fluid Mech 603:39–61

Porteiro JLF (1986) Wake periodicity in subsonic bluff-body flows. AIAA J 24:1703–1704

Porteiro JLF, Perez-Villar V (1996) Wake development in turbulent subsonic axisymmetric flows. Exp Fluids 21:145–150

Porteiro JLF, Przirembel CEG, Page RH (1983) Modification of subsonic wakes using boundary layer and base mass transfer. AIAA J 21:665–670

Rind E, Castro IP (2012) On the effects of free-stream turbulence on axisymmetric disc wakes. Exp Fluids 53:301–318

Roshko A (1954) On the drag and shedding frequency of two-dimensional bluff bodies. NACA Technical Note 3169

Rowe A, Fry ALA, Motallebi F (2001) Influence of boundary-layer thickness on base pressure and vortex shedding frequency. AIAA J 39:754–756

Sakamoto H, Haniu H (1990) A study on vortex shedding from spheres in a uniform flow. J Fluids Eng 112:386–392

Sevilla A, Martinez-Bazan C (2004) Vortex shedding in high Reynolds number axisymmetric bluff-body wakes: local linear instability and global bleed control. Phys Fluids 16:3460–3469

Thiria B, Cadot O, Beaudoin JF (2009) Passive drag control of a blunt trailing edge cylinder. J Fluid Struct 25:766–776

Vilaplana G, Grandemange M, Gohlke M, Cadot O (2013) Global mode of a sphere turbulent wake controlled by a small sphere. J Fluid Struct 41:119–126

Viswanath PR (1996) Flow management techniques for base and afterbody drag reduction. Prog Aerosp Sci 32:79–129

Walsh MJ (1990) Riblets. In: Bushnell DM, Hefner JN (eds) Viscous drag reduction in boundary layers. Progress in astronautics and aeronautics, vol 123. AIAA, Washington, pp 203–261

Weickgenannt A, Monkewitz PA (2000) Control of vortex shedding in an axisymmetric bluff body wake. Eur J Mech B Fluids 19:789–812

Whitmore SA, Naughton JW (2002) Drag reduction on blunt-based vehicles using forebody surface roughness. J Spacecr Rockets 39:596–604

Williamson CHK (1996) Vortex dynamics in the cylinder wake. Annu Rev Fluid Mech 28:477–539

Wu JC (1981) Theory for aerodynamic force and moment in viscous flows. AIAA J 19:432–441

Wu JZ, Ma HY, Zhou MD (2006) Vorticity and vortex dynamics. Springer, Berlin

Wygnanski I, Fiedler HE (1970) The two-dimensional mixing region. J Fluid Mech 41:327–361